RSC Advances

ARTICLE

Insufficient oxygen diffusion leads to distortions of microbial growth parameters assessed by isothermal microcalorimetry

T.Maskow[a], F. Mariana Morais[a], L. F. M. Rosa[a], Y.G. Qian[b] and F. Harnisch[a]

Heat is directly related to the number of bacteria as well as the kinetics and stoichiometry of bioconversions. Approximately 100 000 aerobically growing bacteria or 100 myocardial cells produce generally enough heat being measurable in conventional isothermal microcalorimeters in real time. The most convenient method to measure heat signals are isothermal microcalorimetry (IMC) experiments using closed unstirred ampoules in multichannel instruments. The convincing advantages of this simple method led to many applications in medicine, pharmacy, environmental sciences and control of food and tap water. However, serious concerns for the characterization of biological processes arise from the often unclear influence of potential oxygen depletion on the heat signal. In this article we show that oxygen bioavailability shapes the heat signal of IMC measurements significantly. Therefore, the balance between oxygen sink (microbial activities) and oxygen source (diffusion from gas phase) in relation to the spatial biomass distribution is quantitatively evaluated here for the first time. Thereby it is demonstrated that the oxygen bioavailability is a limiting factor for several IMC measurements. Based on these results, practical suggestions for calorimetric experiments with lower influence of oxygen bioavailability are derived. As rule of thumb, only the heat trace up to 95 J L^{-1} at 37 $^{\circ}$C should be evaluated, if there should be no influence of oxygen diffusion, for the study of homogenously distributed biomass. Furthermore, experimental measures to reduce the influence of oxygen bioavailability on the heat signal are discussed.

1. Introduction

Metabolism can be considered as an array of biochemical reactions, involving the conversion of chemical energy to thermal energy. Thus, microbial growth is reflected by exothermic and - in one exception - endothermic heat flux[1]. To measure heat fluxes, the most simple and frequently applied method is isothermal microcalorimetry (IMC) using ampoules as reaction vessels. IMC allows up to 48 parallel experiments with a current detection limit of 5×10^{-5} W per liter reaction volume, corresponding to 200 nW of heat flux when using a 4 mL ampoule[2]. This tiny heat flux equals ~~to~~ a microbial oxygen depletion of air saturated medium (approx. 6.7 mg L^{-1} at 37 $^{\circ}$C) within 44 days. Considering glucose as example of carbon and energy source, this correlates to the diminutive consumption rate of 0.03 μM h^{-1} or 6 μg L^{-1} h^{-1}, assuming complete

microbial glucose combustion[3]. This extraordinary sensitivity in combination with the possibility of high-throughput measurements qualifies IMC for applications in different fields of research and routine analysis. For medical research the exploitation of IMC is inter alia reported for the detection of contaminations of donated blood platelets [4, 5], ultra-fast determination of inhibitory effect of antibiotics [6-8] and Chinese natural medicine [9], the distinction of methicillin-susceptible from methicillin-resistant *Staphylococcus aureus* [10, 11], and the fast determination of bacterial growth on implants or other biomedical surfaces [12]. Further applications in medical research are summarized in a good review by Braissant et al.[13]. Calorimetry is also widely applied in environmental microbiology, for instance for the fast determination of microbial degradation kinetics [14] even for pollutants in trace concentrations [15]. Using IMC the activity of the soil biota can be quantified [16] and the

influence of predators or bacteriophages on the microbial community can be assessed [17, 18]. In food research calorimetry can be applied for fast determination of bacterial contaminations in tap or table water [19]. Overviews about the exploitation of IMC in environmental microbiology are given by Rong et al. [14] and in food industry by Wadsö and Galindo [20]. The convincing advantage of IMC applications are the simplicity of sample preparation and the measurement sensitivity. Briefly, the sample solution, e.g. containing the microbial inoculate in a nutrient broth, is placed in an ampoule being closed before starting the measurement and thus forming a closed compartment composed of a liquid phase and gas phase [21] (for details see Fig. S1 in the supplementary material). Nowadays, the application range of IMC measurements is extended to the addition of reactants (e.g. nutrients, antibiotics, predatory bacteria or phages) during the experimental run to the calorimetric ampoule allowing examining the interaction of these compounds[22].

The simplicity of the practical measurement of IMC may mask two possible weaknesses, which are often ignored while interpreting calorimetric (routine) measurements. The first limitation results from the often observed sedimentation of the biological material and the resulting heterogeneity. However, sedimentation can be avoided by adjusting the density of the measurement solution to the density of the biological entity under study using metabolically inactive substances [23]. Alternatively, defined conditions can be assured by locating the biological material on solid, floating surfaces [24]. The second limitation is caused by changing concentrations of nutrients and other reacting compounds, during the measurement. Most important is the proton formation or consumption, leading to pH-shifts, and the oxygen consumption during aerobic respiration. Whereas pH-shift can be counterbalanced by using media with sufficient buffer capacity, the changing oxygen availability, however, is a more severe issue. This is mainly due to the very low solubility of oxygen in aqueous solutions (approx. 6.7 mg/L at 37 $^{\circ}$C and 101.325 kPa)[25].

In response to limited oxygen availability numerous microorganisms shift from respiratory to fermentative metabolism. Noteworthy, the related growth reaction enthalpy is often twenty times higher for respiratory than for fermentative metabolism [26]. Therefore the potential for oxygen limitation has to be considered for IMC-data, to avoid misinterpretation of growth stoichiometry and kinetics. In principle, in addition to the oxygen contained in the medium solution, oxygen can be delivered from the head space of the

ampoule to this solution by diffusion. However, the diffusivity of oxygen in water is low [27]. Therefore in this article we exploit experiments as well as modelling strategies to gain better insights on the O_2-limitation during IMC and to develop strategies to overcome this limitation. It is shown that oxygen transport does play a limiting role for most IMC measurements and thus affect the thermal signal. We also show that easy-to-handle methods allowing minimizing the length of the diffusion pathway of O_2 exist.

2. Experimental

2.1 Test organisms, media, and precultivation

Pseudomonas putida MM1 as an example for a strictly aerobic microorganism (DSM 9278, obtained from Deutsche Sammlung von Mikroorganismen und Zellkulturen, Braunschweig, Germany) was used to analyse the influence of oxygen diffusion on the heat signal. *P. putida* was cultivated on Tryptic Soy (TS) medium (made of CASO agar from Carl Roth GmbH+Co. KG, Karlsruhe, Germany) by transferring a colony from the agar plate into an Erlenmeyer flask containing 20 mL of this medium. The liquid cultures were incubated overnight on rotation shaker (150 rpm) at 25 ± 0.2 $^{\circ}$C. The bacteria used as inocula were harvested from active cultures right before the calorimetric experiments.

2.2 Determination of growth rate

The specific growth rate of the microorganisms was determined under related experimental conditions. For this, an overnight liquid culture was transferred into an Erlenmeyer flask containing 50 mL of fresh TS medium. The initial optical density at 700 nm (UV-Vis Spectral Photometer Hitachi U-2900, Hitachi High-Tech, Tokyo, Japan) was set to 0.1. The culture was incubated on a rotation shaker (150 rpm) at 25 ± 0.2 $^{\circ}$C. Every hour 1 mL sample was taken for optical density measurement. The logarithmic plot of the optical density vs. time delivered the maximum specific growth rate.

2.3 Determination of oxygen concentration profiles

The determination of oxygen concentration in the ampoule was carried out with a fibre optic oxygen microsensor (PreSens – Precision Sensing GmbH, Regensburg, Germany) connected to Microx TX3 transmitter from the same company. The sensor was calibrated prior to the measurements using two-point calibration principle (100% value was measured in fresh oxygen saturated TS medium; 0% value was measured in TS medium mixed with sodium dithionite). Two mL of an overnight preculture was centrifuged at

10000 rpm for 10 min. The supernatant was discarded and a small part of the cell pellets was diluted in 2 mL fresh TS medium prepared in a calorimetric ampoule. The numbers of the cell pellets were varied to achieve optical densities of 0.1 and 0.2. The micro-sensor was located 1 cm below the liquid surface and the oxygen measurement was started immediately. The data were collected at an interval of every 5 s until the oxygen depleted.

2.4 Calorimetric measurements

All experiments were conducted in Thermal Activity Monitor III (TAM III, TA Instruments, New Castle, USA). The ampoules and caps were autoclaved (30 min, 121 °C) and the ampoules serving as reaction vessel filled as described in the respective experiment. The electric gain calibration was regularly performed.

2.5 Respirometry

High performance respirometry (Oxograph-2k, Oroboros Instruments, Innsbruck, Austria) was used to quantify the parameter of eq. 1 (half saturation constant, k_O, and maximum oxygen consumption rate, r_{max}). For that purpose the measuring chambers were filled with TS medium. Later, *P. putida* was added to different optical densities (OD_{700} from 0.02 - 0.22) and the measuring chamber was closed air tight. The chamber interior was stirred (750 rpm), the temperature kept constant at 25 °C and the oxygen concentration monitored by a Clark electrode with a frequency of 0.5 s^{-1}. The data was transferred to OriginPro 8.5G and processed for parameter fittings. The Monod-like Eq. 1 describes the dependency of oxygen consumption rate, r_{O2}, on oxygen concentration O.

$$r_{O2} = r_{O2}^{Max} \frac{O}{k_O + O} \qquad (1)$$

The maximum oxygen consumption rate, r_{O2}^{Max}, and half saturation constant k_O are parameters depending on the bacterial strain as well as growth conditions. They were obtained by fitting O vs. r_{O2}. r_{O2} was determined by numerical differentiation of the experimentally determined oxygen concentration vs. time profile (using a Savitzky-Golay polynomial of the order 2 and a window of 20 points). The parameter fitting of different respirometric experiments to Eq. 1 yields the parameter $k_O = (1.68\pm0.32)\times10^{-3}$ mmol/L. The replicates at 5 different biomass concentrations (OD_{700} 0.02 – 0.22) were done and evaluated.

2.6 Simulations

For consideration of the combined influence of diffusion and metabolic activity a finite element method (FEM) approach was implemented in COMSOL Multiphysics. The geometry was a simplified 2D (bi-dimensional) representation of a calorimetric ampoule (10 x 20 mm for the liquid phase and 10 x 20 mm for the gas phase). Equilibrium of oxygen in air and liquid phase was assumed. The meshing was optimized and a final mesh of 6504 triangles and 1080 quadrilateral elements was used to discretize and solve the partial differential equations for transport. The fluid dynamics were not considered for these simulations, because calorimetric ampoules are not stirred. Preliminary estimations (data not shown) indicate that the dynamics due to convective heat transfer can be neglected. Eq. 2 is the balance equation considering oxygen accumulation $\partial O/\partial t$, oxygen transport by diffusion $\nabla(-D\nabla O)$, and metabolic oxygen consumption r_{O2}.

$$\frac{\partial O}{\partial t} + \nabla\left(-D\nabla O\right) = -r_{O2} \qquad \text{with}$$

$$\nabla \equiv i\frac{\partial}{\partial x} + j\frac{\partial}{\partial y} + k\frac{\partial}{\partial z} \qquad (2)$$

D, O are diffusion coefficient and oxygen concentration in the liquid phase, respectively. Eq. 2 can be also applied to other components like glucose with the respective diffusion coefficient. The recharging of the liquid surface layer with oxygen is described by Henry's Law (eq. 3).

$$O(X = 0) = k_H \, P_{O2} \qquad \text{with } P_{O2} = \xi^V \, P \qquad (3)$$

k_H, P_{O2}, ξ^V, P are the Henry coefficient, the oxygen partial pressure, the mole fraction of oxygen in the gas phase and the total pressure, respectively. The oxygen sink can be described by eq.1 with the following specification.

$$r_{O2}^{Max} = Y_{O/B} \, B \, \mu_{max} \qquad (4)$$

$Y_{O/B}$, B, μ_{max} are the yield coefficient, biomass concentration and maximum specific growth rate, respectively. $Y_{O/B}$ expresses the moles of oxygen consumed to form "one mole" of biomass. $Y_{O/B}$ can be estimated to be 0.897 for every carbon substrate with a degree of reductance $\leq$ 4.67 using simple stoichiometric and biothermodynamic considerations (see supplementary material). This

holds true for the most usual carbon sources (e.g. all carbohydrates, 70 % of amino acids, proteins, the most organic acids). The biomass concentration B is a representative of the number of bacteria and given in the respective experiment. B was derived from the OD_{700} measurement taking the conversion factor of 0.55 mg/L. The conversion factor was derived from the slope of plotting cell dry weight versus OD_{700}. Cell dry weight was gravimetrically determined (in quadruplicate after oven drying at 105 ∘C). The maximum specific growth rate was determined from the logarithmic plot of OD_{700} of growth curves vs. time.

Many microorganisms are not reliant on oxygen as a terminal electron acceptor. They evolved additionally a fermentative metabolism. For analyzing the oxygen diffusion influence on microorganisms with fermentative and respiratory metabolism a simple mathematical growth model is required describing the transition from respiratory to fermentative metabolism (Eq. 5-8).

$$\mu = \frac{\mu_{Max}^{Aerob} O + \mu_{Max}^{Anaerob} k_O}{k_O + O} \quad \frac{S}{k_s + S} \qquad (5)$$

$$Y_{B/S} = \frac{Y_{B/S}^{Aerob} O + Y_{B/S}^{Anaerob} k_O}{k_O + O} \qquad (6)$$

$$Y_{O/B} = Y_{O/B}^{Aerob} \frac{O}{k_O + O} \qquad (7)$$

$$\Delta_R H_X = \frac{\Delta_R H_X^{Aerob} O + \Delta_R H_X^{Anaerob} k_O}{k_O + O} \qquad (8)$$

S and k_S stand for the concentration and half saturation constant of the growth limiting carbon substrate (glucose). The superscripts indicate the type of metabolism aerobic or anaerobic. These types of equations describe aerobiosis if $O>>k_O$ and the anaerobiosis if $O<<k_O$. The part of aerobiosis on the total metabolism is described by $O/(k_O+O)$ and the part of anaerobiosis by $k_O/(k_O+O)$. All of the applied parameters and their respective source are given in table 1 or described for the respective simulation.

Table 1: Applied parameter for the oxygen simulations (for *P. putida*)

Parameter	Symbol	Value	Dimension	Sources
Diffusion coefficient oxygen	D_O	3.3×10^{-9} (37 ˚C) 2.6×10^{-9} (25 ˚C)	$m^2\ s^{-1}$	[28]
Diffusion coefficient glucose	D_G	0.6×10^{-9}	$m^2\ s^{-1}$	[29]
Henry coefficient	k_H	1.02×10^{-8} (37 ˚C) 1.28×10^{-8} (25 ˚C)	mol L^{-1} Pa^{-1}	[30]
Half saturation constant	k_O	$(1.68 \pm 0.32)\ 10^{-3}$ (25˚C)	mol m^{-3}	Respirometric measurements
Mole fraction oxygen in air	ξ^V	0.2095	---	[31]
Maximum specific growth rate	μ_{MAX}	0.19 ± 0.02 (25 ˚C)	h^{-1}	Growth experiments
Oxygen concentration air	O^V	8.232 (37 ˚C) 8.563 (25 ˚C)	mol m^{-3}	Calculated from ideal gas law
Atmospheric pressure	P	101 325	Pa	CRC handbook
Yield coefficient	$Y_{O/B}$	0.897	mol mol^{-1}	Considerations in S1

3. Results and discussion

3.1 Influence of oxygen availability on strictly aerobically respiring microorganisms

First, the simplest case of a microorganism which grows strictly aerobic is investigated using *Pseudomas putida* as model. *P. putida* was grown in a calorimeter ampoule i) under strictly anaerobic conditions (2 mL headspace and 2 mL liquid containing the bacterial suspension of the ampoule is flushed with N_2 before the experiment), ii) under aerobic conditions in closed ampoules (2 mL aerated bacterial suspension and 2 mL air filled head space) and iii) under aerobic conditions in a stirred ampoule with air headspace (calorimetric vessel for isothermal titration experiments; 2 ml aerated bacterial suspension). Fig. 1 shows the respective heat patterns. The calorimetric data are provided as heat, Q, instead of as heat flow, P, as only the reaction heat ($Q = \int P\ dt$) can be related to the expected heat using the oxycaloric equivalent of -460 kJ/mol-O_2.
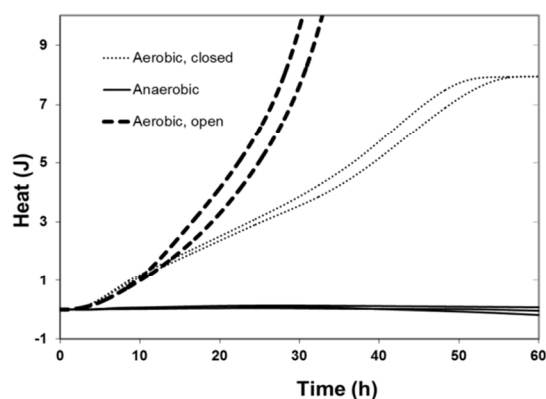
Figure 1: Growth of *P. putida* on TS medium under different conditions at 25 °C (details see text).

Due to the inability of *P. putida* to grow in the absence of oxygen, the observation of zero heat production under anaerobic conditions fits the expectations perfectly. For the experiments employing the closed, air filled ampoules the following can be stated. When considering the oxycaloric equivalent of – 460 kJ of heat produced per mole of consumed oxygen for aerobic respiration [32], the maximum metabolic heat resulting from i) the respiration of the dissolved oxygen in the liquid phase (0.25 J; 5.43×10^{-7} mol-O_2) or ii) all oxygen (dissolved oxygen and oxygen in the head space 8.13 J; 1.77×10^{-5} mol-O_2) in the ampoule can be estimated. The experimentally determined heat (8.0±0.1 J) indicates that all available oxygen is metabolically consumed (8.13 J) and the growth is finished due to oxygen depletion. The heat in stirred and open calorimetric vessel increased to values > 10 J indicating that significantly more energy is available for conditions not limited by oxygen availability. The slope of the signals, i.e. the heat production rate P, was similar for the first hours for both aerobic conditions. This indicates that only at beginning of the experiment the heat production (i.e. growth rate) was depending on the respective properties of the organism and for the later phase the oxygen diffusion governed the heat signal. This is a very important finding for the evaluation of the analytical potential of the IMC with closed ampoules.

3.2 Influence of oxygen diffusion on the heat signal of microorganisms

As shown above, the measured heat signal is strongly dependent on the oxygen availability. As a consequence, for most IMC experiments the heat signal is therefore determined by a balance between oxygen transport from the headspace to the solution in the ampoule and the metabolic oxygen consumption. Therefore the oxygen concentration time profiles were investigated. The time course of the oxygen concentration was predicted using a finite element approach (for details see materials and methods) and assessed experimentally for different biomass concentrations. Fig. 2 compares calculated and measured oxygen concentration profiles at two different initial biomass concentrations.
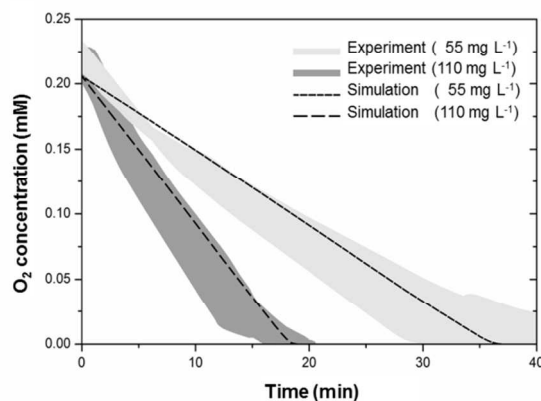

Figure 2: Comparison of measured and modelled oxygen concentration in calorimetric ampoules. The measuring probe was immersed 1 cm in the culture broth and experimental results show the error range of three different measurements.

As Fig. 2 illustrates, the simulated values correspond well with the measured data, indicating that the model described the processes properly. Thus, more complex systems that include, for instance, non-homogenous distribution of biomass were investigated *in-silico*. Respective simulations for biomass accumulated as sediment in the ampoule or concentrated on the top layer (in both cases as a 0.5 mm layer) are shown in Fig. 3.
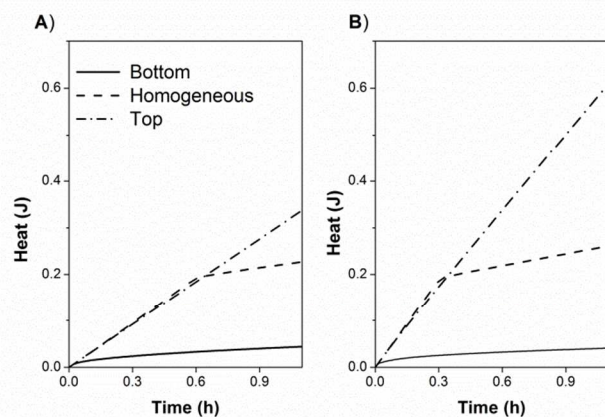
Figure 3: Influence of the location of the biomass (on bottom, homogeneously distributed, or on top). The initial biomass concentration was 55 mg/L (A) and 110 mg/L (B), respectively. All other parameters are summarized in table 1.

Fig. 3 illustrates that for homogenously distributed biomass or for biomass sedimented on the bottom of the calorimetric ampoule oxygen diffusion becomes growth governing very rapidly (for sedimented biomass independent on the biomass concentration at 0.2 h; for homogenously distributed biomass: B = 55 mg/L at 0.6 h; B = 110 mg/L at 0.3 h). As shown by the third scenario, concentrating the biomass on top of the liquid phase, e.g. on a floating disk, can solve the problem of oxygen limitation. Biomass flotation can be also achieved by increasing the media density based on addition of inert materials, e.g. colloidal silica particles coated by polyvinylpyrrolidone (Percoll) [33]. Percoll is known not to penetrate biological membranes [34]. To further validate that Percoll does not contribute to any metabolic and non-metabolic signals the heat flux of mixtures of five different amounts of Percoll with living and dead bacteria and with sterile medium was calorimetrically monitored. In the experiments with living 110 mg L^{-1} *P. putida* only decay curves with a total heat of 1.16 ± 0.09 J after 60 h were measured. In the experiments with dead bacteria and without bacteria a final heat of 0.17 ± 0.07 J and 0.00 ± 0.02 J were determined, respectively (results not shown). These results demonstrate clearly that the interaction of Percoll with dead cells and with the medium can be neglected, when analyzing the heat signals on their biological meaning. If the density of the Percoll suspension is higher than the density of the bacterial cells, the cells are concentrated near the interface between the liquid

and gas phase of the ampoule. To confirm the hypothesis that the influence of Percoll on medium density and distribution of biomass indirectly reduces the influence of oxygen diffusion, the growth of *P. putida* was measured calorimetrically for different Percoll concentrations (Fig. 4). Furthermore, the heat evolution was modelled assuming that the biomass is concentrated in the top layer of the liquid phase forming a 0.5 mm thick film at the liquid surface.
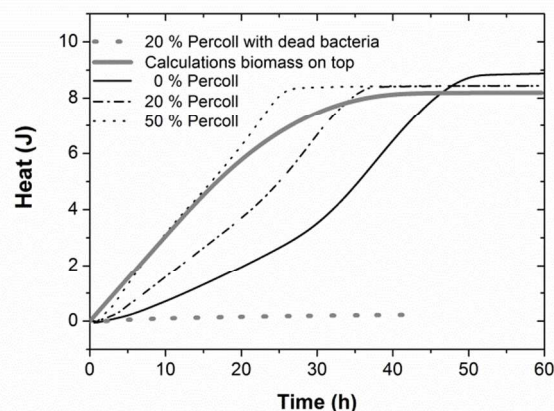

Figure 4: Influence of Percoll on growth of *P. putida* on TS medium at 25 °C (details see text).

The slopes of heat vs. time (proportional to the oxygen consumption rate) increased with the presence of Percoll, which matched the expectation that the diffusion path was reduced. Assuming a total consumption of all oxygen in the ampoule, a total heat of approx. 8.13 J should be observed independent of the experimental conditions. This was confirmed as the measured final heat for all set-ups was 8.70 ± 0.61 J (6 measurements with 5 different Percoll concentrations). Finally, the highest measured heat production rate – reflected as slope of heat vs. time in Figure 4 (89 µW, at 50% Percoll) – fits perfectly to the simulation results (85 µW), when assuming that the biomass is concentrated in the top layer of the liquid phase. Altogether these results support the hypothesis that the oxygen availability does limit the metabolic activity for strict aerobic microorganism in IMC-measurements. These findings also demonstrate that for strictly aerobically respiring microorganisms the growth kinetics, but not the total heat production, is a function of oxygen diffusion.

In general, the simulations of oxygen availability show that the oxygen concentration in the growth media decreases very fast, if the biomass is distributed homogeneously or located on the bottom of

the ampoule. What happens if microorganisms possess an extreme high affinity to oxygen or an extreme low half saturation constant k_O? Following eq. 1, the oxygen consumption rate becomes virtually independent of the oxygen concentration. Thus, the question arises, if microorganisms could overcome oxygen limitations by metabolic reactions possessing extreme low k_O? It is difficult to study the influence of extreme high affinity (i.e. very low k_O) by solving eq. 2 numerically. However, it is possible to solve eq. 2 analytically in 1 D, when assuming steady state conditions ($\partial O / \partial t = 0$) (see supplementary material for details). The solution is shown in eq. 9 and reads as:

$$X = \sqrt{\frac{2D}{Y_{O/B} \, X \, \mu_{max}} \left(k_O \ln\left(\frac{O}{O_O}\right) + O - O_O \right)}$$

$$(9)$$

X, O, O_0 are the depth, the oxygen concentration in the liquid phase and the oxygen concentration on the top of the liquid phase (X=0), respectively. Based on eq. (9), it can be surprisingly shown that the oxygen affinity of the microorganisms does not significantly influence the average oxygen concentration ($\int O(X) \, dX$) and the related average oxygen consumption rate (see eq. 4) and heat flux. However, the oxygen profile (O=O(X)) is largely effected. The penetration depth of oxygen is higher for solutions containing microorganisms possessing a low O_2 affinity than it is for solutions containing microorganisms with high affinity. Even the transition between oxic and anoxic ranges in the calorimetric ampoule is smoother, when using microorganisms possessing a low O_2 affinity. (A figure illustrating these effects can be found in the supplementary material.) Note, these estimations do not consider the dynamics of accumulated oxygen consumption, e.g. by increase of biomass or by other transport mechanisms than diffusion like convection. However, they provide a good insight into the effects of oxygen affinity on microbial activity and the resulting oxygen profiles.

3.3 Influence of oxygen bioavailability on organisms with respirative and fermentative metabolism

Many microorganisms are not solely reliant on oxygen based metabolism, but developed different types of fermentative metabolism for oxygen limiting conditions. A hypothetical microorganism was assumed for simulating the influence of oxygen bioavailability on the calorimetric results. The hypothetical microorganism possesses a mixed metabolism determined by the eqs. 5-8 with a maximum specific growth rate of 0.8 h^{-1} for aerobic

metabolism and 0.1 h^{-1} for fermentative metabolism. The yield coefficients are 3.3 mol/mol (aerobic) and 0.84 mol/mol (anaerobic). These are typical values for growth on glucose [35, 36]. Fig. 5 compares the simulated growth patterns without (A) and with (B) taking oxygen diffusion into account. For the simulations biomass concentration of 0.02 mM and glucose concentration of 0.5 mM and oxygen saturated medium at 37 °C at the begin were assumed. The other conditions are given in table 1.
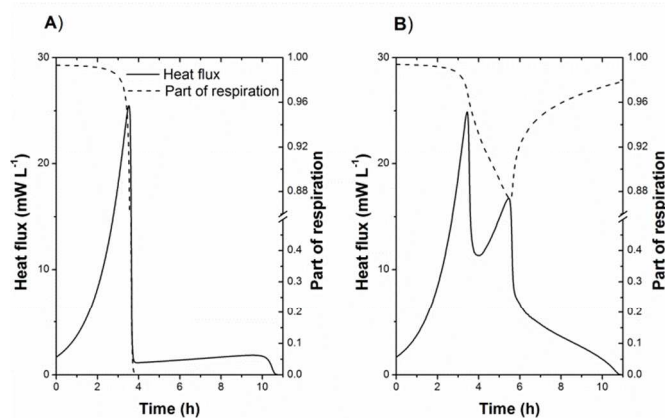

Figure 5: Heat production rate (solid line) and part of respiration on the total metabolism ($O/(k_O+O)$) (dashed line) for the growth of a hypothetical microorganism A) without and B) with oxygen diffusion.

Both simulations show two maxima of the heat flux or, respectively, two growth phases. This is a typical behavior for microorganisms with a mixed metabolism, which was for instance often observed for *E. coli* growing on different media [9, 19, 37]. Without considering oxygen diffusion, the simulated growth was first (up to 4 hours) mainly aerobic and later anaerobic. Growth was finished due to exhaustion of the carbon-substrate. The part of respiration on the total metabolism defined as ($O/(k_O+O)$) was here and in the following taken to allocate the nature of the growth process. Based on the clear discrimination between the aerobic and anaerobic part of growth, the logarithmic plot of the heat flux vs. time should provide the maximum growth rate for the different phases. Indeed, $\mu_{MAX}=0.7919\pm0.0002$ h^{-1} (R=0.99995) was determined for the aerobic phase and $\mu_{MAX}=0.0957\pm0.0001$ h^{-1} (R=0.9995) for the anaerobic phase being in accordance with model input values (aerobic: 0.8 h^{-1} and anaerobic: 0.1 h^{-1}). The derived reaction heat of - 327.1 kJ mol^{-1} glucose corresponds to the expectation of - 336 kJ mol^{-1} assuming that the growth enthalpy is a linear combination of

the aerobic reaction with $\Delta_R H$=-1256.5 kJ mol^{-1} and the fermentative reaction with $\Delta_R H$=-94.0 kJ mol^{-1}. The reaction enthalpies and the share of respiration to total metabolism were calculated from the growth stoichiometry of the hypothetical microorganism. Note that under the measuring conditions the difference between reaction heat and the reaction enthalpy due to potential pressure rise is 4.4 kJ mol^{-1} in the worst case and can thus be neglected. In summary, when the oxygen diffusion does not play a key-role, the calorimetric signal is simply determined by the sequence of metabolic events.

However, a surprising picture arises if oxygen diffusion is considered. As Figure 5 B shows no clear bi-phasic behavior can be detected, the second peak of the heat flux is (compared to Fig. 5A) much higher and shows a long tailing, indicating overlap of aerobic and anaerobic growth during the second growth phase. The logarithmic plot of the first growth phase delivers μ_{MAX}=0.8084±0.0003 h^{-1} (R=0.9999), being in accordance with the model input value of 0.8 h^{-1} for aerobic growth. However, for the seemingly anaerobic growth phase a μ_{MAX}=0.320±0.001 h^{-1} (R=0.9935) was derived. The latter value is approx. three times higher than the model input value of 0.1 h^{-1} for anaerobic growth. The derived reaction heat is, with – 576.8 kJ mol^{-1}, nearly doubled when the diffusion was not taken into account (although diffusion itself does not contribute to heat flux). This finding becomes clear, when considering the share of respiration on the total metabolism. Due to O_2 diffusion from the gas phase the respiration even in the seemingly anaerobic part never became zero. The minimum value was 87 % aerobic and only 13 % anaerobic metabolism during seemingly complete respiration (at time 5.7 h). In general, the simulation results clearly indicate that calorimetric results of IMC based measurements with air in the head space of the ampoule have to be interpreted with care. Of course, also the spatially discretized results of the simulations are interesting and deserve further discussion, being beyond the scope of this paper.

3.4 Consequences

The presented results indicate that only calorimetric measurements that remain below a certain threshold, Q/V, are certainly solely influenced by metabolic events. Q/V is determined by the amount of dissolved oxygen. Above Q/V oxygen diffusion strongly influences or even governs the growth and thus the heat signal. The threshold Q/V is defined by equation 10.

$$Q/V = \Delta H_{OX}\, O_{SL} \qquad (10)$$

ΔH_{OX}, O_{SL} are the oxicaloric equivalent of – 460 kJ mol^{-1} and the dissolved oxygen concentration, respectively. Note that the influence of k_O is neglected in eq. 10, because $O_{SL} \gg k_O$ for most microorganisms. Furthermore, the dependency of oxygen solubility on temperature and salinity of the nutrient broth has to be taken into account. A first approximation of the dissolved oxygen at atmospheric pressure as a function of salinity can be taken from tables[25]. As a rule of thumb the following thresholds in J L^{-1} can be applied for different temperatures: 130 (20 °C), 108 (30 °C), 100 (37 °C). From the practical perspective and for the usual ampoule experiments filled with 2 mL bacterial suspension and 2 mL head space the thresholds in J are: 0.32 (10 °C), 0.26 (20 °C), 0.22 (30 °C), 0.19 (37 °C). These thresholds are obviously not valid for strong anaerobic measurement conditions (e.g. the ampoule is filled in a nitrogen tent and the medium as well as the head space does not contain any oxygen).

3.5 Preventive measure

The threshold is not valid and the influence of oxygen diffusion on the heat signal can be prevented for i) measurements in open, stirred calorimetric vessels (e.g. in isothermal titration instruments), ii) performing the growth reaction outside of the calorimeter and pumping the bacterial suspension through a flow-through calorimeter, iii) homogenization by stirring or shaking of the closed calorimetric ampoule or iv) reduced oxygen diffusion path.

Pumping a microbial suspension from a reaction vessel outside through a flow-through calorimeter was very early matter of calorimeter developments [38]. However, oxygen consumption [39] and ongoing bioprocesses in flow lines [40] as well as clogging can cause distortions. Wadsö proposed in 1997 rocking calorimeters with the intention to mix heterogeneous systems with the tendency to sediment [41]. Wadsö and Li published in 2011 a self-constructed magnetically stirred calorimeter[39]. Both suggestions have the potential to overcome problems of oxygen diffusion influence. In summary, some efforts are required to improve the detection limit of those instruments for experiments with microorganisms. Modern instruments achieve the sensitivity but they are not shaken. Because smooth shaking has no influence on the thermoelectric effect, it is in principle possible to design shaken high sensitive calorimeters. The disturbance by the heat release due to fluid dynamics can be potentially considered by reference measurements..

Even without designing new instruments the influence of oxygen diffusion on calorimetric experiments can be reduced by shortening the diffusion path, e.g. including solutions of high density and floating surface - as discussed above. These solutions have the advantage to be applicable to the already existing multichannel instruments.

Conclusions

Our study demonstrates clearly how important it is to consider oxygen bioavailability in the interpretation of IMC measurements of pure respiratory or mixed respiratory/ fermentative growing microorganisms. We showed that in order to ensure that the measured calorimetric signal is determined by the properties of the organism under investigation, the measurement should be carried out below the threshold value, Q/V, which is determined by the amount of dissolved oxygen. This is very important considering the different applications of IMC, e.g. for monitoring toxic effects, for evaluating the effect of antibiotics or stimulating agents, and for interpreting biological interactions with phages or predatory bacteria. Even thermodynamic data like growth reaction enthalpies will be determined wrongly.

If the experiments cannot be performed below Q/V, the oxygen diffusion path has to be shortened. This can be done by application of shaken or rocking calorimeter or by adding agents to increase the density of the growth medium as shown above.

Acknowledgements

Notes and references

^a UFZ - Helmholtz Centre for Environmental Research, Department of Environmental Microbiology, Permoserstr. 15, 04318 Leipzig, Germany.
^b School of Environmental Studies & Key Laboratory of Biogeology and Environmental Geology of Chinese Ministry of Education & Sino-Hungarian Joint Laboratory of Environmental Science and Health, China University of Geosciences, 430074 Wuhan, PR China.
Electronic Supplementary Information (ESI) available: General applicable $Y_{O/B}$ and analytical solutions of the oxygen balance. See DOI: 10.1039/b000000x/

1. U. von Stockar, *J Non-Equilib Thermodyn*, 2010, **35**, 415-475.
2. TA Instruments, http://www.tainstruments.com, 2014.
3. T. Maskow, T. Schubert, A. Wolf, F. Buchholz, L. Regestein, J. Buechs, F. Mertens, H. Harms and J. Lerchner, *Appl. Microbiol. Biotechnol.*, 2011, **92**, 55-66.
4. K. T. Ripa, P. A. Mardh, B. Hovelius and K. Ljungholm, *J. Clin. Microbiol.*, 1977, **5**, 393-396.
5. A. Trampuz, S. Salzmann, J. Antheaume and A. U. Daniels, *Transfusion*, 2007, **47**, 1643-1650.
6. L. Xi, L. Yi, W. Jun, L. Huigang and Q. Songsheng, *Thermochim. Acta*, 2002, **387**, 57-61.
7. L. Yang, L. X. Sun, F. Xu, J. Zhang, J. Zhao, Z. Zhao, C. Song, R. Wu and R. Ozao, *J. Therm. Anal. Calorim.*, 2010, **100**, 589-592.
8. U. von Ah, D. Wirz and A. Daniels, *BMC Microbiol*, 2009, **9**.
9. W. Kong, J. Wang, X. Xiao, S. Chen and M. Yang, *Analyst*, 2012, **137**, 216-222.
10. U. von Ah, D. Wirz and A. Daniels, *J. Clin. Microbiol.*, 2008, **46**, 2083-2087.
11. D. Baldoni, H. Hermann, R. Frei, A. Trampuz and A. Steinhuber, *J. Clin. Microbiol.*, 2009, **47**, 774-776.
12. I. Hauser-Gerspach, P. S. de Freitas, A. U. Dan Daniels and J. Meyer, *J Biomed Mater Res B Appl Biomater*, 2008, **85**, 42-49.
13. O. Braissant, D. Wirz, B. Göpfert and A. Daniels, *Sensors*, 2010, **10**, 9369-9383.
14. X.-M. Rong, Q.-Y. Huang, D.-H. Jiang, P. Cai and W. Liang, *Pedosphere*, 2007, **17**, 137-145.
15. F. Mariana, F. Buchholz, H. Harms, Z. Yong, J. Yao and T. Maskow, *J Microbiol Methods*, 2010, **82**, 42-48.
16. N. Barros, J. Salgado, J. Rodríguez-Añón, J. Proupín, M. Villanueva and L. Hansen, *J. Therm. Anal. Calorim.*, 2010, **99**, 771-777.
17. F. Buchholz, J. Lerchner, F. Mariana, U. Kuhlicke, T. R. Neu, H. Harms and T. Maskow, *Biofouling*, 2012, **28**, 351-362.
18. L. Guosheng, L. Yi, C. Xiangdong, L. Peng, S. Ping and Q. Songsheng, *J. Virol. Methods*, 2003, **112**, 137-143.
19. T. Maskow, K. Wolf, W. Kunze, S. Enders and H. Harms, *Thermochim. Acta*, 2012, **543**, 273-280.
20. L. Wadsö and F. Gómez Galindo, *Food Control*, 2009, **20**, 956-961.
21. O. Braissant, D. Wirz, B. Goepfert and A. U. Daniels, *FEMS Microbiol. Lett.*, 2010, **303**, 1-8.
22. T. Manneck, O. Braissant, Y. Haggenmuller and J. Keiser, *J. Clin. Microbiol.*, 2011, **49**, 1217-1225.
23. A. J. Fontana, L. D. Hansen, R. W. Breidenbach and R. S. Criddle, *Thermochim. Acta*, 1990, **172**, 105-113.
24. M. Astasov-Frauenhoffer, O. Braissant, I. Hauser-Gerspach, R. Weiger, C. Walter, N. U. Zitzmann and T. Waltimo, *Journal of periodontology*, 2013, 1-10.
25. U.S. Department of the Interior / U.S. Geological Survey, http://water.usgs.gov/owq/FieldManual/Chapter6/6.2.4.pdf, 2013.
26. U. von Stockar, L. Gustafsson, C. Larsson, I. Marison, P. Tissot and E. Gnaiger, *Biochim. Biophys. Acta*, 1993, **1183**, 221-240.
27. W. Hayduk and H. Laudie, *AIChE J.*, 1974, **20**, 611-615.
28. J. Grote, *Pflügers Archiv*, 1967, **295**, 245-254.
29. A. C. F. Ribeiro, O. Ortona, S. M. N. Simões, C. I. A. V. Santos, P. M. R. A. Prazeres, A. J. M. Valente, V. M. M. Lobo and H. D.

RSC Advances Accepted Manuscript

Burrows, *Journal of Chemical & Engineering Data*, 2006, **51**, 1836-1840.

30. J. A. Dean, ed., *Lange's Handbook of Chemistry*, McGraw-Hill, Inc., 1992.

31. S. Kshudiram, ed., *The earth's atmosphere - its physics and dynamics.*, Springer, Berlin, 2008.

32. E. Gnaiger and R. B. Kemp, *Biochim. Biophys. Acta*, 1990, **1016**, 328-332.

33. H. Pertoft, T. C. Laurent, T. Lååsa and L. Kågedala, *Anal Biochem*, 1978, **88**, 271-282.

34. H. Pertoft, K. Rubin, L. Kjellén, T. C. Laurent and B. Klingeborn, *Exp. Cell Res.*, 1977, **110**, 449-457.

35. U. von Stockar, ed., *Biothermodynamics The Role of Thermodynamics in Biochemical Engineering*, EPFL Press, Lausanne, 2013.

36. L. M. Wick, H. Weilenmann and T. Egli, *Microbiology*, 2002, **148**, 2889-2902.

37. J. Antheaume, S. Salzmann, A. Steinhuber, R. Frei, A. Daniels and A. Trampuz, *International Journal of Antimicrobial Agents*, 2007, **29**, S22-S22.

38. A. Beezer, R. Newell and H. Tyrrell, *Antonie van Leeuwenhoek*, 1979, **45**, 55-63.

39. L. Regestein, A. Wolf, H. J. Schneider, T. Maskow, F. Mertens, J. Büchs and J. Lerchner, *Thermochim. Acta*, 2012, **544**, 10-16.

40. T. Maskow, D. Olomolaiye, U. Breuer and R. Kemp, *Biotechnol. Bioeng.*, 2004, **85**, 547-552.

41. I. Wadsö, *Chem. Soc. Rev.*, 1997, **26**, 79-86.

42. L. Wadsö and Y. Li, *J. Chem. Educ.*, 2011, **88**, 101-105.